Proceedings of the
Annual Stability Conference
Structural Stability Research Council
St. Louis, Missouri, April 2-5, 2019

Influence of the length of patch load on the ultimate load of longitudinally stiffened plate girders

Sasa Kovacevic[1], Nenad Markovic[2]

Abstract

An experimental-numerical analysis regarding the ultimate strength of longitudinally stiffened I-girders subjected to concentrated loading is presented. The driving force for this research was to investigate the influence of patch load length on ultimate capacity of longitudinally stiffened girders. In order to assess the patch loading resistance of plate girders, a nonlinear finite element analysis has been performed. The numerical results are compared with the experimental tests using different patch load lengths. For a better verification with the experimental results, the finite element model includes the experimentally measured initial geometrical imperfections and material properties based on the laboratory tests. It has been shown that the numerical and experimental results are in perfect agreement which enabled a fruitful background for parametric analysis, in which different initial geometrical imperfections have been used to ameliorate understandings about their influence on the ultimate load under different patch load lengths. Conclusively it may be stated that initial geometrical imperfections can play a decisive role, especially for stiffened girders. Initial geometrical imperfections of stiffened girders that correspond to deformed shapes at collapse (collapse-affine imperfections), will give the most unfavorable ultimate strengths. In the present paper, the third buckling mode of stiffened girders corresponds to the deformed shape and the lowest ultimate strengths are obtained. Future experimental and numerical work will consider the effects of different geometry, material characteristics and aspect ratio of web plate.

1. Introduction

A plate girder is a beam built up of steel plates and shapes to form a deep flexural member that can support greater loads on longer spans which cannot be economically carried by standard rolled beams. Besides a myriad of advantages, one of the most important demerits of plate girders is susceptibility to buckling since they consist of a combination of thin plates. Patch load is a special load case where plate girders are subjected to a concentrated load or partially distributed load. The ultimate strength is achieved by the appearance of web local buckling (web crippling) in the zone of load introduction and deformation of the loaded flange (Fig. 1).

[1] Graduate Teaching Assistant, School of Mechanical and Materials Engineering, Washington State University, <sasa.kovacevic@wsu.edu>
[2] Assistant Professor, Faculty of Civil Engineering, University of Belgrade, <nenad@grf.bg.ac.rs>

Thin-walled steel girders often appear as structural elements which can be loaded in different ways. Except for deep crane runway beams loaded by crane wheels, a remarkable realistic load case in which this situation arises is the launching phase of multi-span steel and composite bridges during construction over temporary or permanent supports. The patch load, in this case, appears by means of high reaction forces of a roller acting on the bottom flange. As the load changes continuously in these situations, transversal stiffeners cannot be efficiently used. Since bridge girders are commonly reinforced by longitudinal stiffeners (cf. Fig. 2a) in order to increase the bending and shear resistance, it is beneficial to consider their influence on girders behavior under the patch load. Therefore, the usage of longitudinal stiffeners for patch load phenomenon is recommendable instead of increasing the web thickness and better knowledge of the behavior of longitudinally stiffened plate girders is extremely important in order to achieve safer and economical designs.

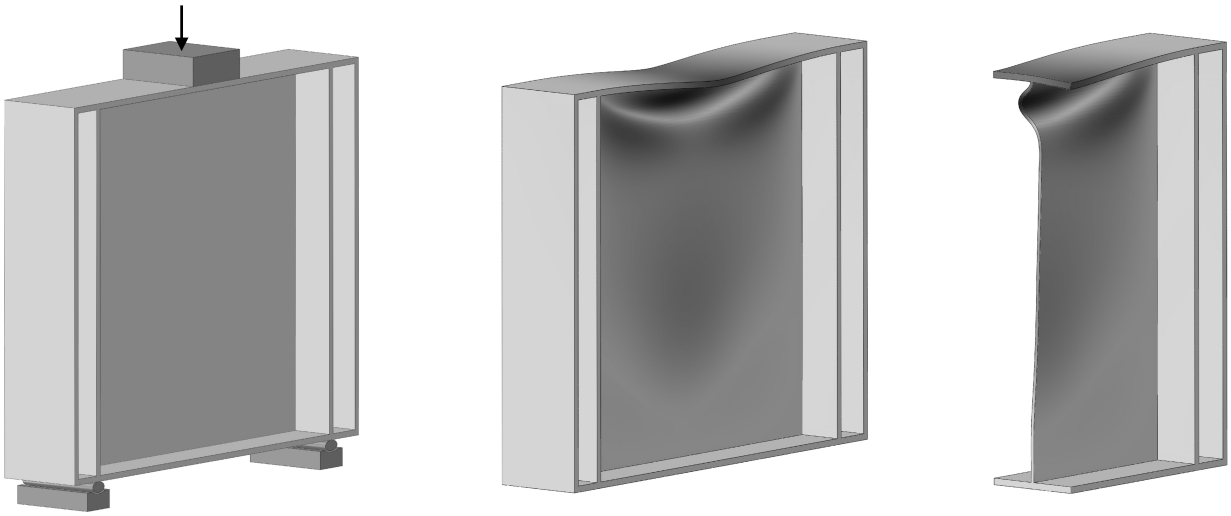

Figure 1: A thin-walled plate girder subjected to localized edge load (patch loading) and typical failure mode

The latest edition of the AISC Specification (ANSI/AISC, 2016) includes a procedure for the determination of ultimate strength of unstiffened girders solely. The procedure is based on the experimental work conducted by (Roberts, 1981a). However, the Specification states that a three-quarter depth transversal stiffener (or stiffeners) or a doubler plate is needed to eliminate web crippling, where the stiffener depth was defined based on research by (Salkar, et al., 2015).

The current European design standard Eurocode 3 (EC3 Part 1-5, 2006) provides a design methodology for the determination of patch loading resistance of both longitudinally stiffened and unstiffened webs. The methodology is originally proposed by (Lagerqvist, 1995) for unstiffened webs while the effect of longitudinal stiffening is adopted according to the work conducted by (Graciano, 2002). Although the design code gives the design procedure for both groups of girders, there is still a need for further development. New improvements of the design standard are proposed by (Davaine, 2005) and (Chacon, et al., 2010). Therefore, in order to provide more design recommendations for ultimate strength of longitudinally stiffened I-girders, it was concluded that an additional experimental and numerical analysis is required.

The main objective of this work is an experimental and numerical investigation of the influence of patch load length and initial geometrical imperfections on the ultimate capacity of

longitudinally stiffened I-girders. The driving force for the research was the fact that a scarce work has been found in literature for the influence of patch load length on the ultimate strength of longitudinally stiffened plate girders. A comprehensive literature review of experimental researches is given in our paper (Markovic & Kovacevic, 2019) and proves that the influence of patch load length was not sufficiently explored in the previous experimental studies. The review is summarized here in Table 1 excluding the present experimental investigation. Numerical analyses including imperfection sensitivity studies considering different initial geometrical imperfections are usually conducted under constant patch load lengths (Graciano & Edlund, 2002), (Graciano, et al., 2011), (Chacon, et al., 2011), (Chacon, et al., 2012a) and (Kuhlmann & Seitz, 2004). On the other hand, the patch load length was varied in (Seitz, 2005), (Davaine, 2005), (Maiorana, et al., 2009), (Kövesdi, 2018) and (Loaiza, et al., 2018), but not as a primary parameter.

The paper is organized as follows. The next section briefly presents own experimental results over fourteen tests conducted on I-girders with and without longitudinal stiffeners. The third section gives a basis for numerical modeling and introduces a nonlinear finite element (FE) model that will be employed in the parametric study presented afterward. The numerical model has been verified via comparison with the experimental results and evoked further directions of the research. The parametric analysis regarding the ultimate strength of plate girders, including different patch load lengths and initial geometrical imperfections, is performed in the fourth section and the results are thoroughly discussed. At the end section, conclusions are given along with recommendations for future investigations.

2. Experimental research

Introductorily it was stated that the influence of patch load length practically was not systematically analyzed. After carefully updating the available literature a database that includes 13 experimental studies, with a total of 159 individual tests has been formed. As one can see in Table 1, analyses considering greater rates of patch load length are not presented. That was the driving force for the present experimental investigation and to give a contribution to examining and clarifying the patch load phenomenon.

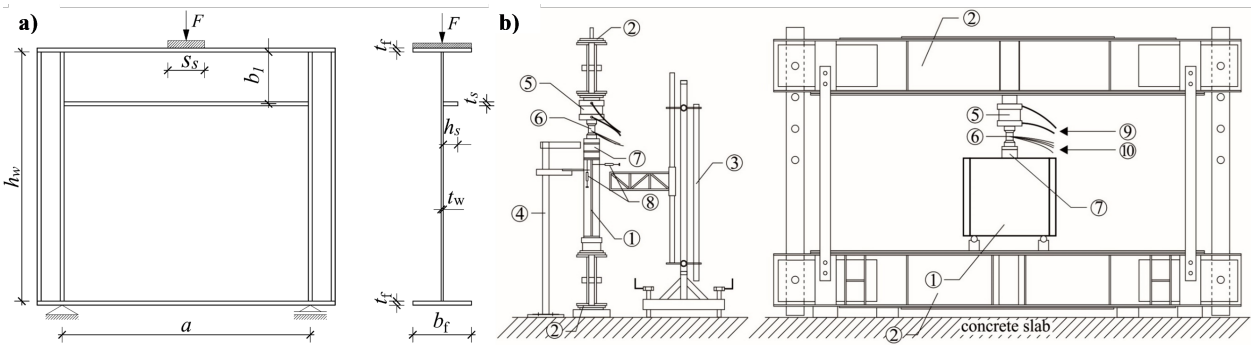

Figure 2: a) Notation used for longitudinally stiffened plate girders subjected to patch loading; b) Schematic view of a girder and used equipment: 1) test girder, 2) closed frame, 3) frame-slider for guiding transducer for the web deformation, 4) frame-slider for holding transducer for the flange deformation, 5) press, 6) load cell, 7) rigid steel block, 8) transducers, 9) pipes for oil supply for hydraulic pump, 10) electrical cables for connection with measuring devices

Table 1: Experimental tests on longitudinally stiffened girders subjected exclusively to patch loading. The present experimental investigation is excluded from the list.

Reference	Number of tests	s_s/a	s_s/h_w	s_s[1] [mm]
(Rockey, et al., 1978)	4	0.05	0.05	40
(Bergfelt, 1979) (Bergfelt, 1983)	15	0.01-0.11	0.05-0.06	40 (13), 120 (2)
(Roberts, 1981b) (Markovic & Hajdin, 1992)	2	0.1	0.1	50
(Oxfort, 1983)	1	0.05	0.08	100
(Shimizu, et al., 1987)	1	0.5	0.3	300
(Galea, et al., 1987)	2	0.39	0.54	690
(Janus, et al., 1988)	101	0.1	0.1-0.2	50 (71), 100 (12), 62 (18)
(Dubas & Tschamper, 1990)	16	0.02-0.14	0.04-0.24	40 (8), 240 (8)
(Dogaki, et al., 1991)	2	0.1	0.1	90
(Salkar, 1992)	2	0.2	0.2	127
(Carretero & Lebet, 1998)	6	0.19-0.25	0.38-0.5	200 (2), 300 (4)
(Walbridge & Lebet, 2001)	5	0.2	0.29	200
(Kuhlmann & Seitz, 2004) (Seitz, 2005)	2	0.58	0.30	700

1. (·) denotes a number of tests for a given patch load length

The present experimental investigation represents an analysis in which the patch load length was varied the most (s_s=0–150 mm, s_s/a=0–0.3, s_s/h_w=0–0.3). The study includes longitudinally stiffened and unstiffened plate girders. The central aim are longitudinally stiffened girders while unstiffened ones are served to provide a reference ultimate strength for the stiffened ones. A total of 14 tests is performed in which 8 girders were longitudinally stiffened with a flat stiffener, placed at b_1=0.2h_w from the loaded flange. Details about the experiments, testing procedure, equipment, experimental results, and findings are thoroughly presented in (Markovic & Kovacevic, 2019) while in this paper only ultimate strengths will be listed. A general notation of a girder is graphically displayed in Fig. 2a while numerical values are summarized in Table 2, including experimentally obtained ultimate capacities (F_{exp}) and material characteristics of the web and flange of each girder (yield stress f_{yw}, f_{yf}, and ultimate tensile stress f_{uw}, f_{uf}).

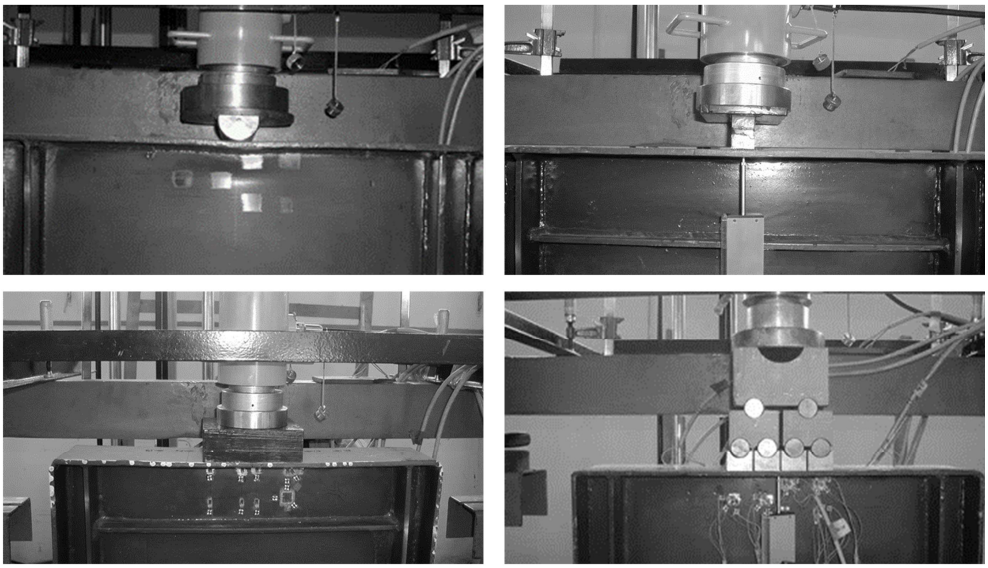

Figure 3: Different load blocks (from left to right): s_s=0, 25, 150 and 4x37.5 mm (even distribution of the load)

The patch load was applied using either a half-round bar (treated as a concentrated force–s_s=0 mm) or rectangular thick steel blocks from 25 mm to 150 mm running the full width of the flange. In order to analyze the influence of stiffness of the loading blocks, additional tests for s_s=150 mm were conducted (girders A13 and A16) using a special system that allows an even distribution of the load over the entire load length. This system was already used in experiments (Lucic, 2003). Characteristic loading blocks are given in Figure 3 while the disposition of the used laboratory is schematically given in Fig. 2b.

Table 2: Ultimate strengths, geometrical and material characteristics of the tested girders

No.	Girder label	a [mm]	h_w [mm]	t_w [mm]	b_f [mm]	t_f [mm]	b_1 [mm]	s_s [mm]	h_s [mm]	t_s [mm]	f_{yw} [MPa]	f_{yf} [MPa]	f_{uw} [MPa]	f_{uf} [MPa]	F_{exp} [kN]
1	A15	500	500	4	120	8	-	0	-	-	327.50	321.00	443.00	468.00	143.30
2	A14	500	500	4	120	8	100	0	30	8	320.50	315.00	441.50	476.00	165.90
3	A12	500	500	4	120	8	-	25	-	-	323.50	321.00	445.00	466.00	154.60
4	A4	500	500	4	120	8	100	25	30	8	320.50	315.00	441.50	476.00	180.00
5	A1	500	500	4	120	8	-	50	-	-	305.00	n.a.[1]	434.00	n.a.[1]	165.00
6	A3	500	500	4	120	8	100	50	30	8	324.00	325.00	437.50	474.00	183.00
7	A17	500	500	4	120	8	100	75	30	8	318.00	317.00	434.00	475.00	194.30
8	A11	500	500	4	120	8	-	100	-	-	305.00	n.a.[1]	434.00	n.a.[1]	199.00
9	A5	500	500	4	120	8	100	100	30	8	327.50	321.00	443.00	468.00	225.00
10	A6	500	500	4	120	8	100	125	30	8	332.00	320.00	444.00	475.00	259.00
11	A2	500	500	4	120	8	-	150	-	-	323.50	321.00	445.00	466.00	215.00
12	A7	500	500	4	120	8	100	150	30	8	318.00	317.00	434.00	475.00	255.00
13	A13	500	500	4	120	8	-	150	-	-	324.00	325.00	437.50	474.00	230.00
14	A16	500	500	4	120	8	100	150	30	8	332.00	320.00	444.00	475.00	244.60
										Average stresses:	321.50	319.83	439.86	472.33	

1. *n.a.*=not available

The force is increased until the ultimate capacity was not exhausted. This was manifested by the appearance of the buckle in the web between the loaded flange and stiffener and rapidly increasing deformations of the web and flange in the zone of load introduction without an increase of load or with a drop of the load. This presents locally loss and local buckling zone is noticed under an applied force. The failure shapes for two girders are shown in Fig. 4.

Figure 4: Failure mode for stiffened girders A4 (s_s=25 mm) and A6 (s_s=125 mm)

According to the obtained ultimate strength, it may be stated that for all tested girders (with and without stiffening) the ultimate capacity was increased with increasing the length of patch load. An increase of patch load length from s_s=0 (half–round bar) to s_s=150 mm produces higher

ultimate capacities more than 50% for both groups of girders. Expectedly, the results follow the tendency, already reported in some tests, that larger loading lengths produce higher increases of ultimate loads, especially for longitudinally stiffened girders due to the presence of longitudinal stiffener. Additionally, the influence of the stiffener can be seen juxtaposing the ultimate load capacities for the stiffened and unstiffened girders. It can be concluded that the first ones have higher ultimate load capacities and that the increase in ultimate capacity is between 6% and 19% (average 13.50%). For a more detailed discussion and conclusions regarding the experimental investigation, the interested reader is referred to (Markovic & Kovacevic, 2019).

3. Nonlinear finite element model

This section presents a nonlinear FE model used in this research. Numerical modeling technique is often employed to effectively expand limited experimental tests and used to scrutinize the influence of relevant parameters connected with a problem. The nonlinear analysis was performed using the commercial multi-purpose finite element software (Abaqus Simulia 2016). All patch loading resistances of the girders were determined using geometrically and materially nonlinear analysis to fully capture the post-buckling behavior. In order to properly and efficiently trace the complex nonlinear path of the load-displacement response of the girders, the modified Riks' method (Riks, 1979) has been used in the FE analysis. This method is an incremental-iterative procedure and it is suitable for predicting unstable, geometrically nonlinear collapses of a structure including nonlinear materials. For a more detailed description of the used FE model see (Kovacevic, et al., 2019).

3.1 Material properties

The numerical model is created taking into account the geometrical and material properties of the plate girders showed in Table 2 (cf. Fig. 2a for general notation). The steel was modeled as an isotropic material with a von Mises yield surface and with an isotropic work hardening assumption. The nonlinear stress-strain relationship was idealized by a multi-linear stress-strain curve assuming hardening up to the ultimate strength of the material. After the ultimate stress was reached, an indefinitely ductile plateau was assumed. For simplicity and to provide relatively general conclusions, one stress-strain curve for the web plate and one for the flange, transversal and longitudinal stiffeners was used in all presented simulations, Fig. 5. They represent a mean curve from the behavior of all uniaxial tests for the webs and flanges. Additionally, in order to define the elastic behavior of the girders, an elastic modulus of 205 GPa and Poisson's ratio of 0.30 is employed.

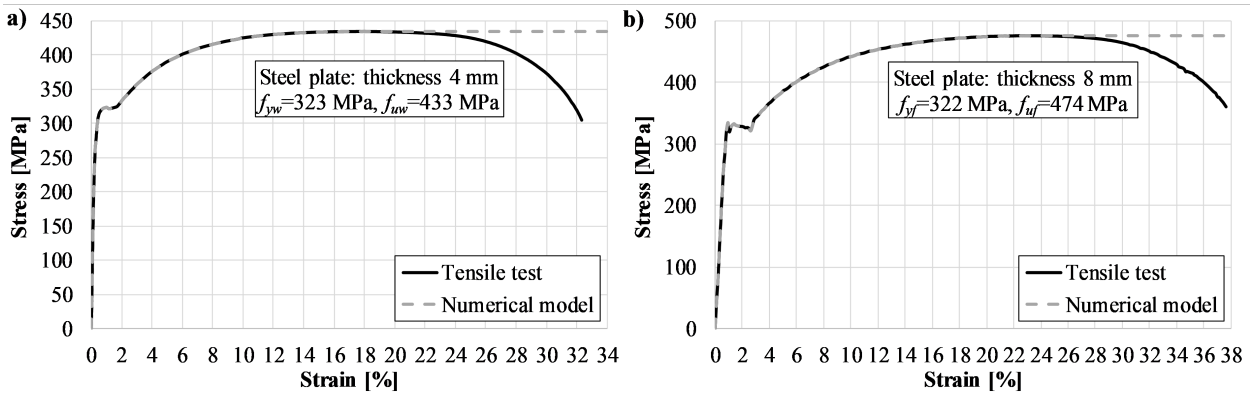

Figure 5: Engineering stress-strain curves for: (a) web plate; (b) flanges, transversal and longitudinal stiffeners

3.2 Loads and boundary conditions

The loading blocks have width b_f and length s_s and they were modeled as rigid regions to ensure rigid behavior perpendicular to the flange surface. The load block for an even distribution of the load over the entire load length (special load block for s_s=150 mm, see Fig. 3), was idealized with 4 independent rigid blocks, cf. Fig 6. This load configuration was only used for comparison with the experimental results (girders A13 and A16) while for the parametric study the load length s_s=150 mm was modeled as one rigid block. A small compressive displacement of 0.5 mm was applied by moving the load blocks towards the upper flange.

The supports were designed as simply supported with symmetrically double-sided transverse stiffeners above them. These nodes are only constrained in the vertical direction. A node at the center of each support is only constrained in the direction perpendicular to the web plane while a node at the center of the girder is only constrained in direction of the girder axis. For the master node, all degrees of freedom are restricted except the vertical direction.

3.3 Finite element mesh

A general-purpose fully-integrated four-node quadrilateral shell element S4 from the Abaqus element library was used for modeling the web, flanges, transversal and longitudinal stiffeners. The rigid loading blocks are modeled as a separate structural element. For all load blocks except for the half-round bar (s_s=0 mm–crane wheel loading), a four–node 3D bilinear rigid quadrilateral element R3D4 was used. In order to generate a more regular finite element mesh with exclusively quadrilateral elements, all girders, and load blocks are meshed using a structured meshing technique with quad and hex element shape control. According to the experimental measurement, the radius of the half-round bar was 25 mm and it was modeled as such. Only for this loading block, a general-purpose fully integrated linear brick element C3D8 was employed. It was also meshed with hexahedral elements and sweep meshing technique is adopted. The girders and load blocks were modeled in full size and the finite element mesh for three representative models is shown in Fig. 6.

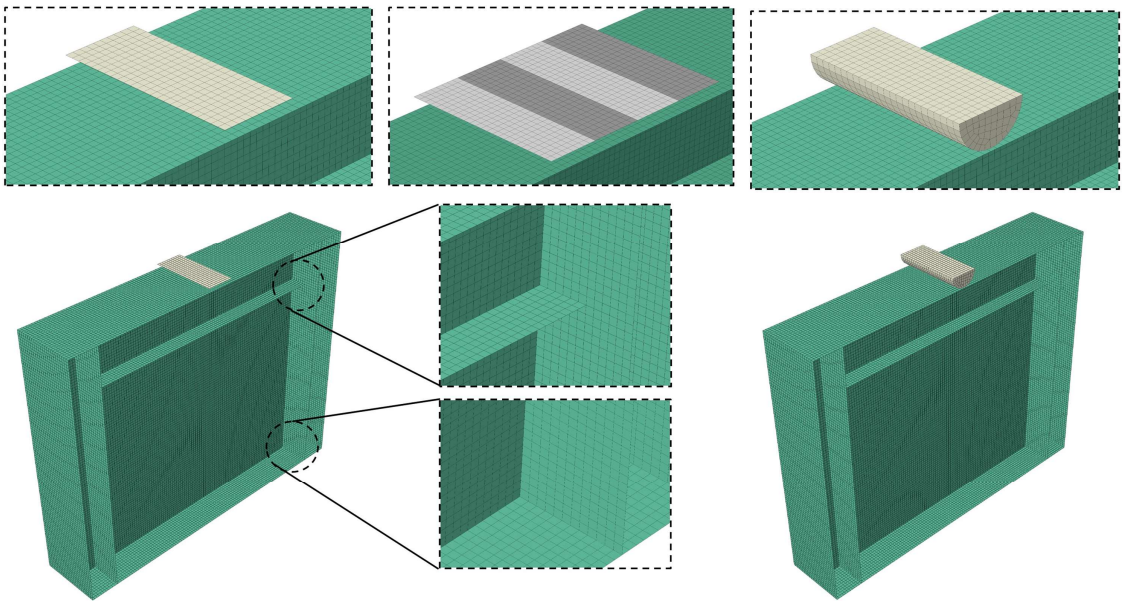

Figure 6: Finite element mesh for three representative models. Rigid blocks for $0<s_s\leq150$ mm (top-left), 4 independent rigid blocks for s_s=150 mm (top-middle) and half-round bar for s_s=0 mm (top-right)

In addition, an *h*-refinement convergence study has been performed for stiffened and unstiffened girders, Fig. 7. One can immediately see that the last two subsequent mesh refinements (from 5 mm to 1.5 mm) do not change the result substantially, e.g. the relative difference for all four girders is around 0.7% but the computational costs are exceedingly increased. Therefore, an element size of 5 mm has been adopted for both groups of girders. The unstiffened and stiffened girders approximately contain 28000 and 30000 finite elements, respectively.

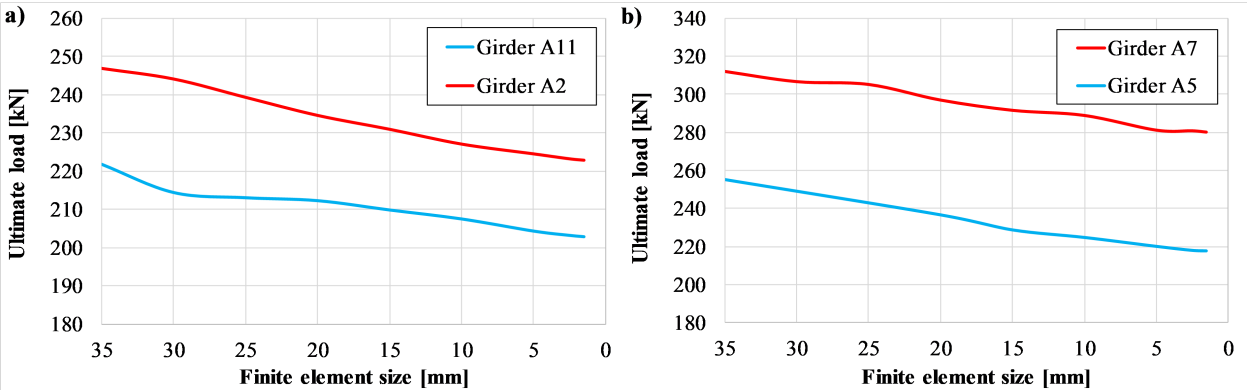

Figure 7: Convergence plot for the ultimate load for: (a) unstiffened girders; (b) stiffened girders

3.4 Initial imperfection

The geometrical initial imperfections are defined by initially imperfect plates following a certain shape. They can be introduced into numerical modeling in different ways, i.e. using experimentally measured imperfections, mode shapes obtained from an eigenvalue buckling analysis or considering imperfections as a two-dimensional random field. For a better validation between the FE model and the experimental results, the experimentally measured web imperfections were used. Those imperfection shapes can be found in (Markovic & Kovacevic, 2019).

Modeling technique for experimentally measured web imperfections is illustrated in Fig. 8. Firstly, all web imperfections are recorded as 3D points (x, y, z coordinates) before each test using a uniform-spaced grid pattern (50x50 mm). Secondly, the point-wise web imperfections are imported into the commercial CAD software (Rhinoceros 2018) in order to define a NURBS surface. The surface is sketched from the grid of points that lie on the surface using second order interpolation functions in both directions and imported into Abaqus. Contrary to the webs, all other elements of the girders, i.e. the flanges, transversal and horizontal stiffeners, were modeled as perfect straight surfaces.

On the other hand, structural imperfections, which are characterized by a residual stress pattern defined by design codes, were not considered since they do not play a decisive role as reported in (Granath, 1997) and (Chacon, et al., 2012b) for unstiffened girders. Also, any flaws concerning unintended rotation of the loaded flange by the load application were not included.

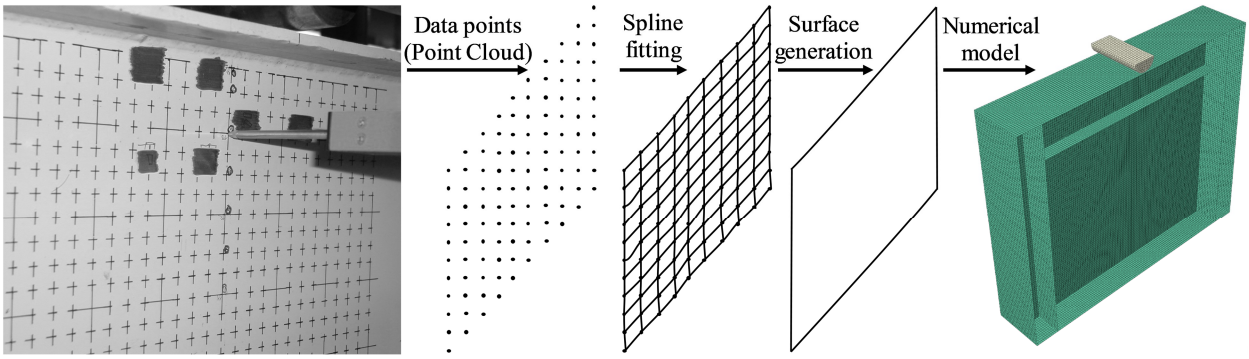

Figure 8: Modeling technique for measured initial geometrical imperfections

3.5 Model verification

In order to investigate the problem further by means of parametric study, the above described FE model will be juxtaposed with the experiment. Table 3 shows a comparison summary of the numerically (F_{FEA}) and experimentally (F_{exp}) obtained patch loading resistance. The present numerical model exhibits a remarkably close agreement with the experimental results with an average error of 0.83% and 2.60% for the unstiffened and stiffened girders, respectively. One should bear in mind that all numerical simulations included the same material characteristics (cf. Fig. 5) and small discrepancies between the results are expected.

Table 3: Experimentally and numerically obtained results of the patch loading resistance [kN]

Unstiffened girders	A15 s_s= 0 mm	A12 s_s= 25 mm	A1 s_s= 50 mm		A11 s_s= 100 mm		A2 s_s= 150 mm	A13 s_s= 150 mm (even distr.)[1]
F_{exp}	143.30	154.60	165.00		199.00		215.00	230.00
F_{FEA}	142.73	144.32	166.02		204.18		224.53	242.35
F_{exp}/F_{FEA}	1.00	1.07	0.99		0.97		0.96	0.95
Stiffened girders	A14 s_s= 0 mm	A4 s_s= 25 mm	A3 s_s= 50 mm	A17 s_s= 75 mm	A5 s_s= 100 mm	A6 s_s= 125 mm	A7 s_s= 150 mm	A16 s_s= 150 mm (even distr.)[1]
F_{exp}	165.90	180.00	183.00	194.30	225.00	259.00	255.00	244.60
F_{FEA}	148.09	156.89	174.58	193.09	227.13	251.78	281.25	254.71
F_{exp}/F_{FEA}	1.12	1.15	1.05	1.01	0.99	1.03	0.91	0.96

1. special load block for an even distribution of the load over the entire load length-see Fig. 3

As a further comparison, the elastoplastic behavior and load-displacement response (vertical displacement of the loading node and normalized capacity) of the experimentally tested girders and numerical simulations will be addressed. For the sake of brevity, the elastoplastic behavior only for stiffened girder A3 (s_s=50 mm) will be considered. As can be seen in Fig. 9, the yielding starts at about 50% of the maximum load, which is in full compliance with the discussion addressed in (Markovic & Kovacevic, 2019). The load-displacement response will be presented only for two different patch load length s_s=50 mm and s_s=100 mm for both stiffened and unstiffened girders, Fig. 10. Those plots also support the findings from the experiments and show a linear behavior up to at least 80% of the ultimate load. In addition, plotting the load-displacement response for longitudinally stiffened and unstiffened girders on the same scale clearly shows the difference in the behavior of stiffened and unstiffened webs. One can instantaneously see that nonlinearities for the longitudinally stiffened girders occur for higher

loads and that the behavior after the ultimate strength is reached can be the same as for unstiffened webs. For a more detailed comparison analysis, see (Kovacevic, et al., 2019).

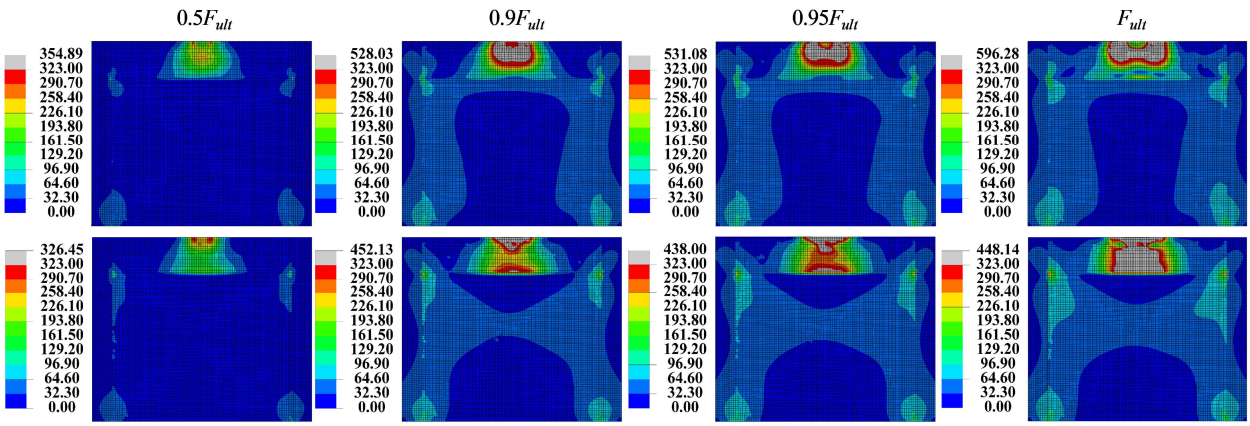

Figure 9: von Mises stress contour plots [MPa] for stiffened girder A3 (s_s=50 mm) at different levels of the ultimate load. The contour plots at the top represent stresses in the shell surface facing the reader (longitudinal stiffener's side) while the bottom plots represent the other surface

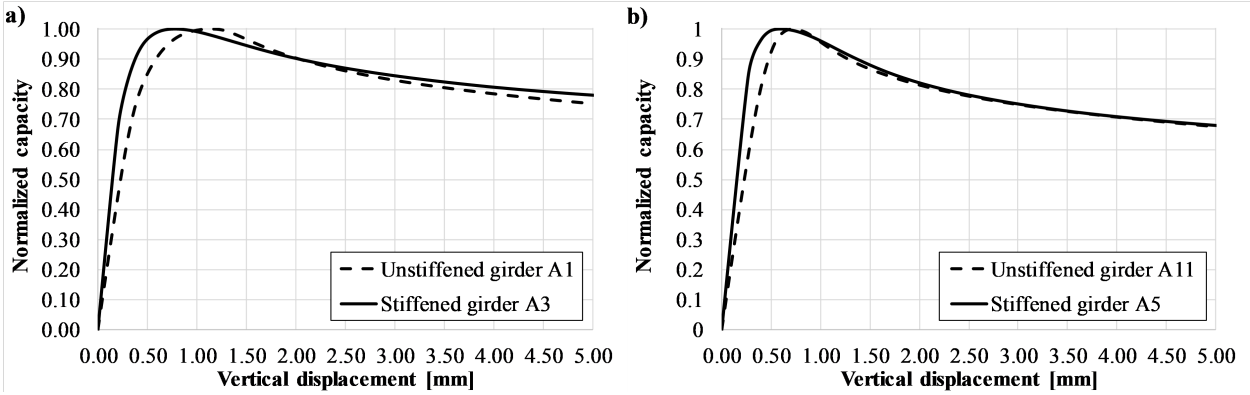

Figure 10: Load-displacement response for unstiffened and stiffened girder under the patch load length of: (a) s_s=50 mm; (b) s_s=100 mm

Conclusively it may be stated that the numerical and experimental results, as well as elastoplastic and load-displacement behavior, are in perfect agreement. The presented FE modeling technique and verification of the model with the experimental results enabled a fruitful background for parametric analysis in which a large number of numerical tests will be developed.

4. Parametric study

Since the presented numerical model has been proved to be valid and accurate for describing the behavior and ultimate strength of the experimental tests, a further set of numerical analyses is performed to investigate the influence of patch load length. The parametric study is formulated with the aim of examining the influence of patch load length considering different shapes of initial geometrical imperfections which was impossible through the experimental program.

To get a better visual picture of the ultimate capacity of longitudinally stiffened girders, the patch load length was varied from 0 mm to 250 mm (s_s/h_w=s_s/a=0–0.5) while the geometrical characteristics (Table 2) and material properties (Fig. 5) were kept constant. In addition, the

position of the longitudinal stiffener (b_1=0.2h_w) was also kept constant even though it is well-known that this position is not the most efficient one for patch loading (Graciano & Edlund, 2002), (Seitz, 2005) and (Graciano & Casanova, 2005). It is recommended by design codes as the optimum location to increase the ultimate strength of plate girders subjected to in-plane bending moments, which is the most present load case for practical purposes. Thus, considering the position of longitudinal stiffeners only to patch loading may give an uneconomical design.

4.1 Numerical results

The present numerical base contains 360 runs, and all numerically obtained ultimate loads for unstiffened and stiffened girders are listed in Table 4 and 5, respectively. In order to exclude the amplitude size, the initial geometrical imperfections are normalized so that the maximum out-of-plane deformation in the upper half of a girder is h_w/100=5 mm, which is within the allowable tolerance in (EC3 Part 1-5, 2006).

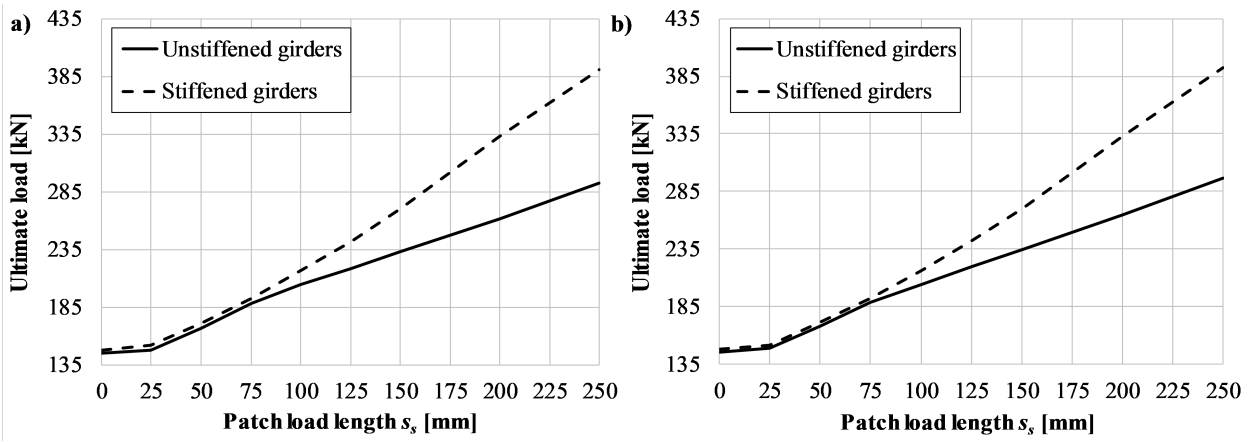

Fig. 11. Ultimate load for longitudinally stiffened and unstiffened girders using normalized initial geometrical imperfections from girder: (a) A11; (b) A12

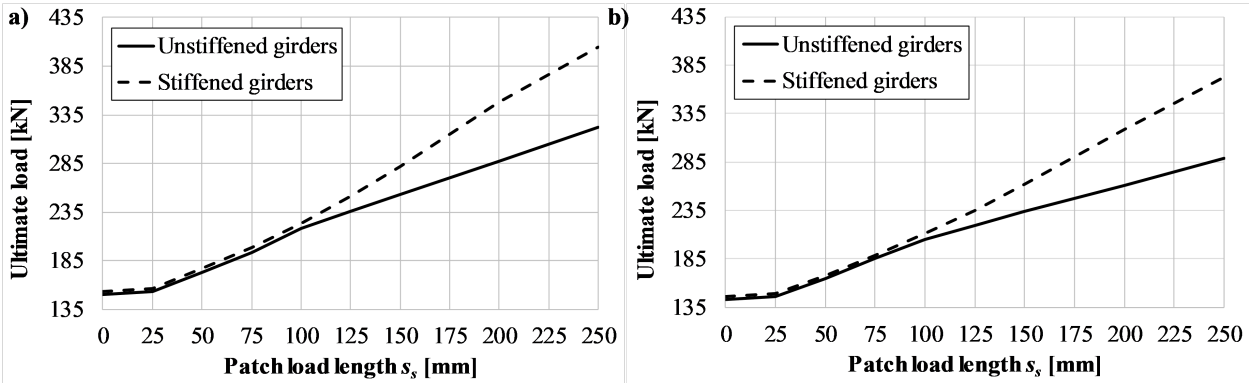

Fig. 12. Ultimate load for longitudinally stiffened and unstiffened girders using normalized initial geometrical imperfections from girder: (a) A7; (b) A14

Different shapes of initial geometrical imperfections are taken into account. Firstly, the experimentally measured initial geometrical imperfections are considered and used for both unstiffened and stiffened girders. These shapes are given in (Markovic & Kovacevic, 2019). For the sake of brevity, patch load resistance for only two girders of each group will be presented graphically, i.e. Fig. 11 shows ultimate strength for two girders experimentally tested as

unstiffened while Fig. 12 gives ultimate strength for two girders experimentally tested as stiffened. A more detailed report is provided in (Kovacevic, et al., 2019). One can instantaneously notice that for smaller patch load lengths the influence of the longitudinal stiffener is negligible and a certain threshold (patch load length) exists after which an appreciable strengthening effect can be achieved.

Secondly, the most used initial geometrical imperfections represent mode shapes based on a linear buckling analysis. A general trend is to use the first three buckling modes and/or their combinations (Chacon, et al., 2009) and (Graciano, et al., 2011), so the same approach will be used in this paper. The first three buckling modes for five different patch load lengths for longitudinally stiffened webs are presented in Fig. 13. The attained results are graphically shown in Fig. 14 and Fig. 15 while numerical values are tabulated in Table 4 and Table 5.

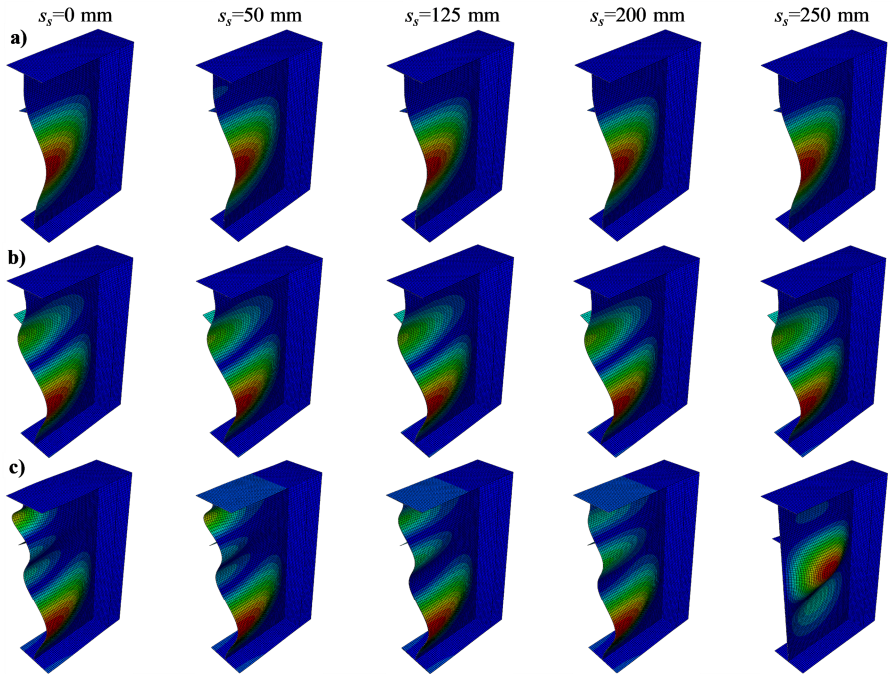

Fig. 13. Buckling modes for longitudinally stiffened girders for different patch load lengths: (a) 1st mode; (b) 2nd mode; (c) 3rd mode

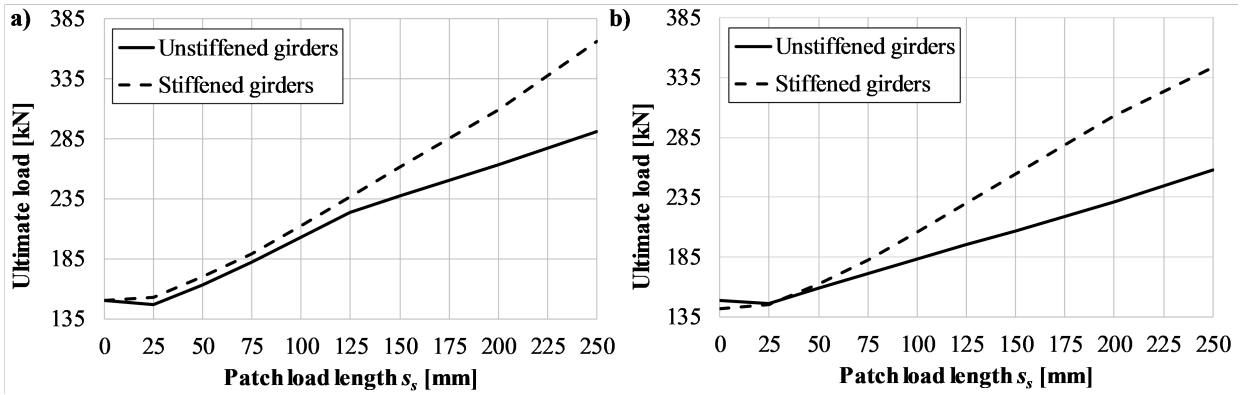

Fig. 14. Ultimate load for longitudinally stiffened and unstiffened girders using initial geometrical imperfections from buckling mode: (a) 1st mode; (b) 2nd mode

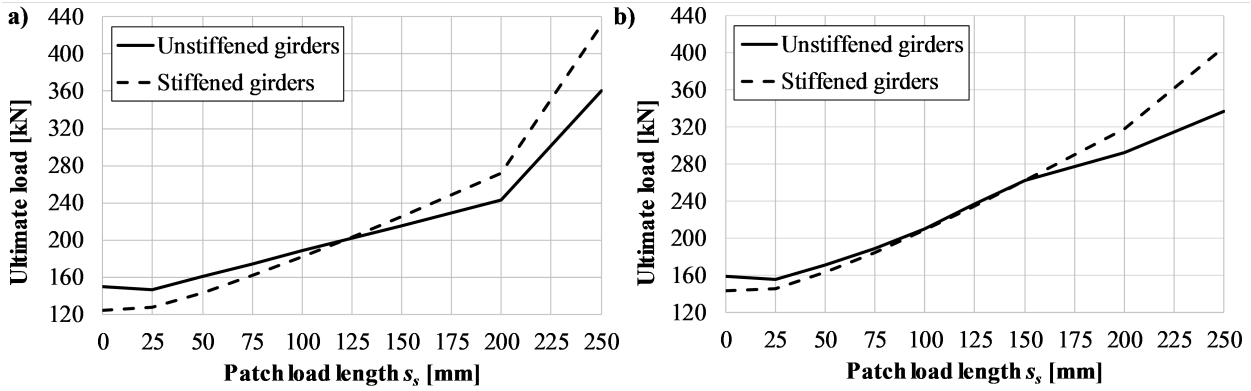

Fig. 15. Ultimate load for longitudinally stiffened and unstiffened girders using initial geometrical imperfections from buckling mode: (a) 3rd mode; (b) combination of the 1st, 2nd and 3rd mode

Thirdly, the initial geometrical imperfections are defined as a two-dimensional random field, usually defined with a sine (Graciano & Casanova, 2005), or cosine function (Granath & Lagerqvist, 1999), (Graciano & Edlund, 2002), (Loaiza, et al., 2018) in both directions (longitudinal and transversal). A schematic view showing the difference between these two imperfections is given in Fig. 16. The obtained results considering these functions are plotted in Fig. 17 and listed in Table 4 and Table 5.

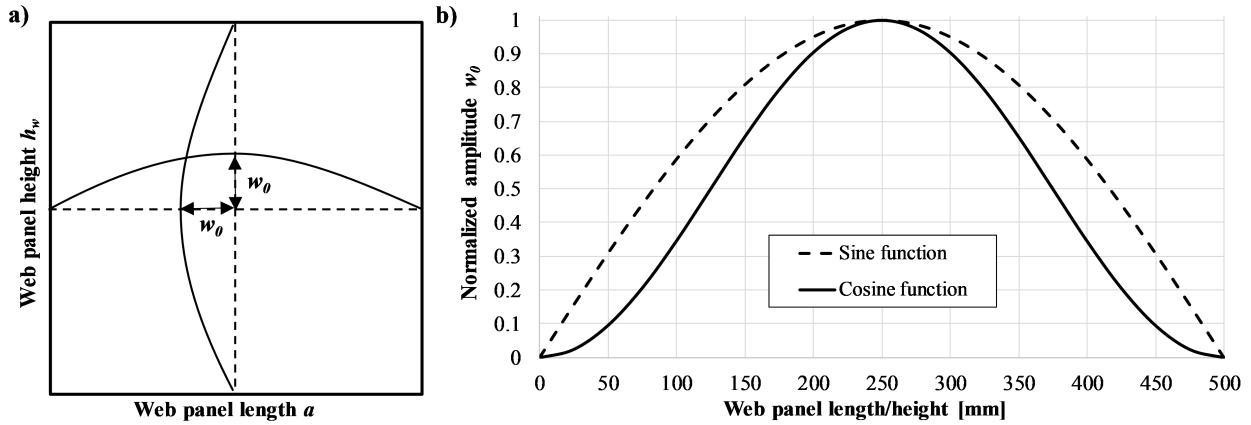

Fig. 16. a) Schematic view of initial shape imperfections modeled using sine and cosine functions; b) midline profile along web panel length/height for sine and cosine function

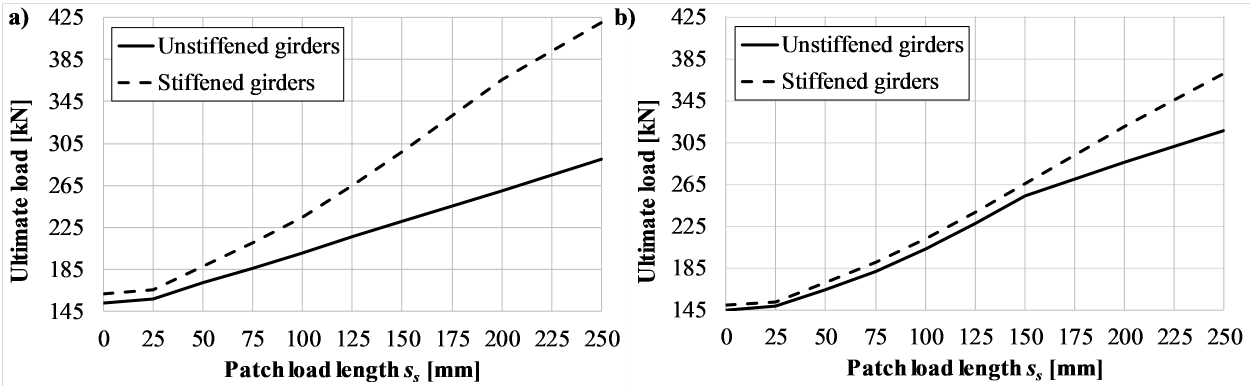

Fig. 17. Ultimate load for longitudinally stiffened and unstiffened girders using initial geometrical imperfections as: (a) sine function; (b) cosine function

Table 4: Numerically obtained patch load resistance for longitudinally unstiffened plate girders [kN]

Shape of initial geometrical imperfection	s_s/h_w								
	0	0.05	0.1	0.15	0.2	0.25	0.3	0.4	0.5
A1	142.68	146.20	164.84	179.82	193.07	206.87	220.42	248.12	280.56
A2	142.82	146.13	165.14	185.47	200.17	214.03	227.86	255.51	285.03
A3	138.56	141.11	153.76	169.04	184.79	200.78	218.58	258.27	300.94
A4	146.35	149.72	168.66	189.82	209.02	223.95	239.14	268.11	298.28
A5	148.78	152.14	170.06	189.67	212.71	234.51	250.64	280.64	311.12
A6	147.98	151.26	168.80	188.01	210.10	236.13	260.58	291.62	322.04
A7	150.20	153.75	173.03	193.79	218.06	235.40	253.55	287.54	322.37
A11	144.68	148.05	166.99	187.97	204.18	218.70	233.23	261.76	292.12
A12	145.25	148.63	167.69	188.79	204.54	219.60	234.73	264.58	296.66
A13	146.29	149.82	169.54	191.29	208.57	224.66	240.63	271.73	304.31
A14	143.04	146.25	164.46	185.00	205.45	219.94	233.65	260.53	289.25
A15	140.44	143.70	161.28	174.98	187.94	200.93	213.76	239.91	268.02
A16	144.45	147.43	163.95	182.47	203.88	228.99	253.59	283.58	314.33
A17	142.25	145.62	165.08	182.13	195.38	208.98	222.29	248.79	276.94
1^{st} buckling mode	150.24	146.58	163.14	182.19	203.05	223.99	237.50	263.25	291.11
2^{nd} buckling mode	149.01	146.03	158.65	171.09	183.37	195.32	206.99	230.98	257.71
3^{rd} buckling mode	149.91	146.76	160.64	174.07	188.19	201.97	215.48	243.50	360.12
$1^{st} + 2^{nd} + 3^{rd}$ mode	159.31	155.39	171.52	188.59	210.22	236.69	262.29	292.35	337.10
Sine function	153.35	157.05	172.60	185.72	201.24	216.32	230.80	259.49	289.96
Cosine function	144.62	147.74	163.63	181.12	202.51	227.12	253.78	285.54	316.08

Table 5: Normalized patch load resistance of longitudinally stiffened plate girders–$F_{stiffened}/F_{unstiffened}$

Shape of initial geometrical imperfection	s_s/h_w								
	0	0.05	0.1	0.15	0.2	0.25	0.3	0.4	0.5
A1	146.56	150.27	170.87	193.46	217.85	244.11	271.80	334.78	389.70
A2	145.58	149.03	168.28	189.77	213.29	238.39	265.39	326.60	385.32
A3	147.18	149.84	165.58	183.64	204.59	226.51	249.06	295.09	339.79
A4	149.31	152.89	172.51	193.81	217.68	240.03	276.06	333.32	388.14
A5	152.05	155.71	175.30	195.96	219.87	246.79	276.84	336.64	389.35
A6	151.24	154.85	174.21	194.85	218.42	244.93	274.16	331.30	381.07
A7	153.05	156.83	177.39	198.95	223.70	251.30	282.04	348.32	404.86
A11	147.87	151.53	170.99	192.36	216.26	242.00	270.23	332.73	390.46
A12	148.07	151.64	171.05	192.49	216.49	242.10	270.07	332.84	391.97
A13	149.33	153.03	173.19	195.02	219.35	245.73	274.32	338.38	396.32
A14	145.81	149.19	167.83	188.58	211.14	235.37	261.79	318.70	372.62
A15	144.16	147.84	168.58	191.26	215.49	241.35	268.65	326.65	372.76
A16	147.76	151.10	169.14	188.85	211.51	236.50	262.83	316.51	366.51
A17	145.20	148.74	168.51	190.36	214.08	239.35	266.00	327.04	386.45
1^{st} buckling mode	150.14	152.74	170.07	188.76	212.25	236.94	261.82	309.27	365.60
2^{nd} buckling mode	141.98	145.18	162.80	182.85	205.47	229.73	254.73	302.92	343.35
3^{rd} buckling mode	124.71	127.39	143.77	161.87	181.69	202.92	225.70	272.24	431.90
$1^{st} + 2^{nd} + 3^{rd}$ mode	143.14	145.80	163.76	184.53	208.77	235.13	262.80	318.49	406.12
Sine function	161.85	165.87	187.91	210.35	234.93	265.02	297.29	365.84	420.37
Cosine function	148.77	152.26	170.43	189.63	212.28	237.86	264.75	319.57	370.82

4.2 Discussion

Considering the experimentally measured imperfections two groups of analysis were established. The first group includes the imperfections of the girders that were originally unstiffened in the experiment. According to these results, one can immediately see that the influence of the longitudinal stiffener for $s_s/h_w \leq 0.15$ (s_s=75 mm) is negligible since it increases the ultimate capacity of less than 5%. On the other hand, for larger patch load lengths the longitudinal stiffener increases the patch load resistance significantly, from 30-40% for s_s/h_w=0.5 (s_s=250 mm). The second group involves the imperfections of the girders that were initially stiffened in the experiment. Again, a similar conclusion can be given, and the same threshold $s_s/h_w \leq 0.15$ is valid. However, for some initial imperfections, the threshold has been shifted even up to s_s/h_w=0.30 (s_s=150 mm). Fig. 18 recaps these conclusions. Additionally, using the numerically obtained results for the experimentally measured imperfections listed in Table 4 and Table 5, it can be shown that the shape of initial geometrical imperfections can play a decisive role for both stiffened and unstiffened girders since it affects the ultimate loads of more than 15%, as portrayed in Fig. 19. This is more pronounced for larger patch load lengths while its impact for $s_s/h_w < 0.10$ (s_s=50 mm) is inappreciable (less than 10%).

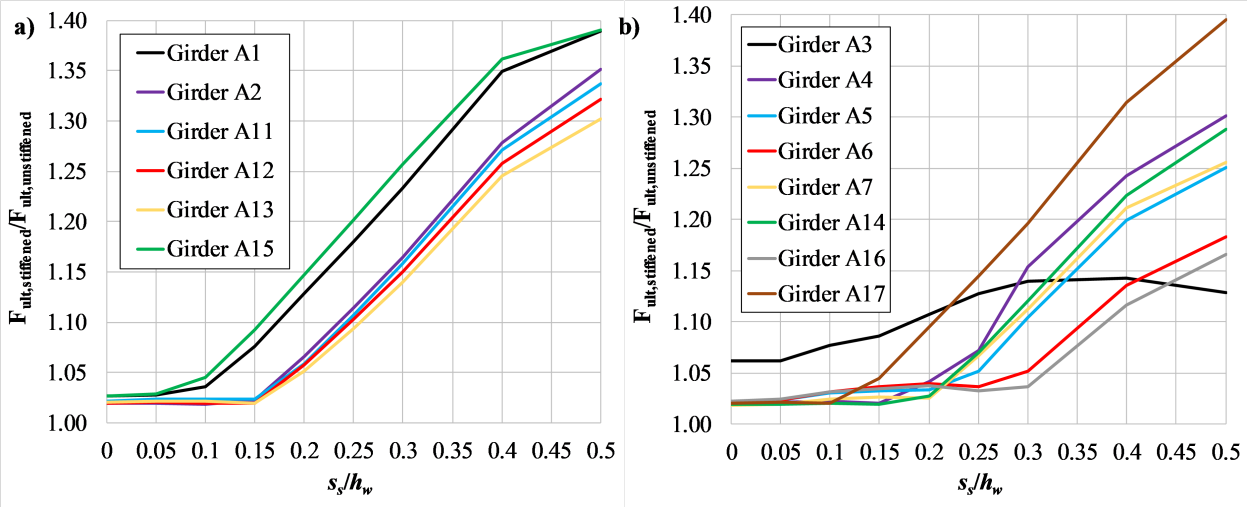

Fig. 18. Normalized ultimate strength for the experimentally obtained initial geometrical imperfections: (a) experimentally unstiffened girders; (b) experimentally stiffened girders

Considering the initial geometrical imperfections defined from an eigenvalues analysis we can confirm the statement from other researchers that the first buckling mode will not give the lowest ultimate strength for both unstiffened and stiffened girders (Graciano, et al., 2011). Furthermore, the first buckling mode gives the same threshold $s_s/h_w \leq 0.15$ (s_s=75 mm) like in the previous case for the experimentally measured imperfections and the difference between the patch load resistance of longitudinally stiffened and unstiffened girders before the threshold is negligible.

In addition, the ultimate strengths for stiffened girders are lower than for unstiffened ones for the third buckling modes and combination of modes ($1^{st}+2^{nd}+3^{rd}$) for $s_s/h_w \leq 0.25$ (s_s=125 mm) and $s_s/h_w \leq 0.30$ (s_s=150 mm), respectively. A similar observation can be noticed for the second buckling mode which, again, gives lower ultimate loads for stiffened than for unstiffened girders only for very small patch load lengths $s_s/h_w \leq 0.05$ (s_s=25 mm). This can be clarified with the shape of the second and third buckling mode for stiffened girders. As can be seen in Fig. 13, the

buckle for these modes of longitudinally stiffened girders occurs between the longitudinal stiffener and loaded flange and its magnitude decreases with increasing the patch load length. As a corollary, this shape of initial geometrical imperfection is much more unfavorable than the second and third buckling mode of unstiffened girders. On the other hand, both the third and combination of modes of stiffened girders give the same increase of 20% for the ultimate loads for s_s/h_w=0.50 (s_s=250 mm) while the maximum increase of 35% is obtained for the second buckling mode. Fig. 20a summarizes these conclusions.

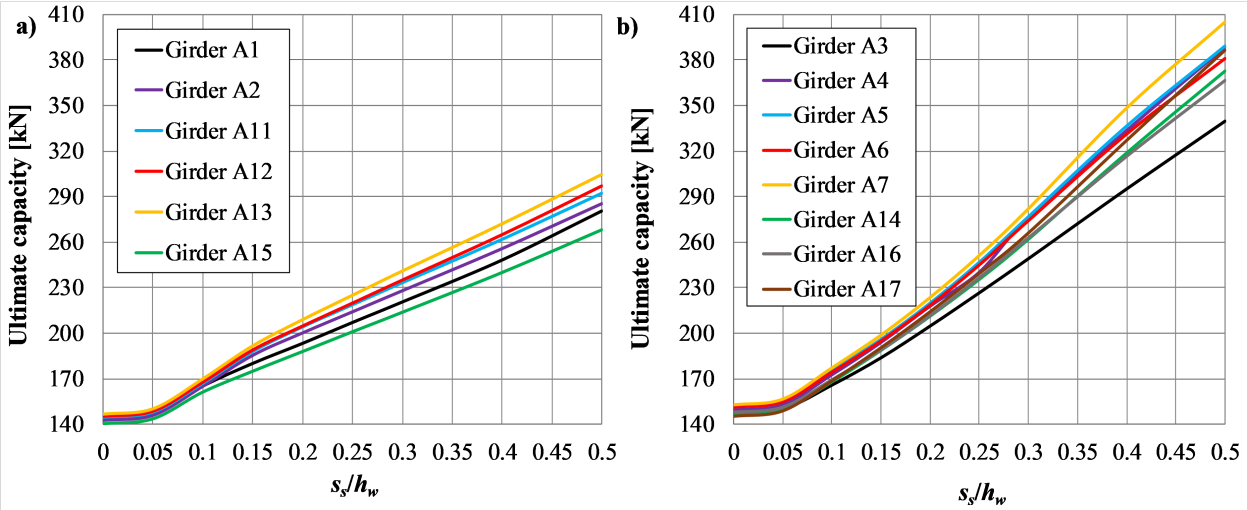

Fig. 19. Ultimate capacity for: (a) unstiffened girders using geometrical imperfections of the experimentally unstiffened girders; (b) stiffened girders using geometrical imperfections of the experimentally stiffened girders

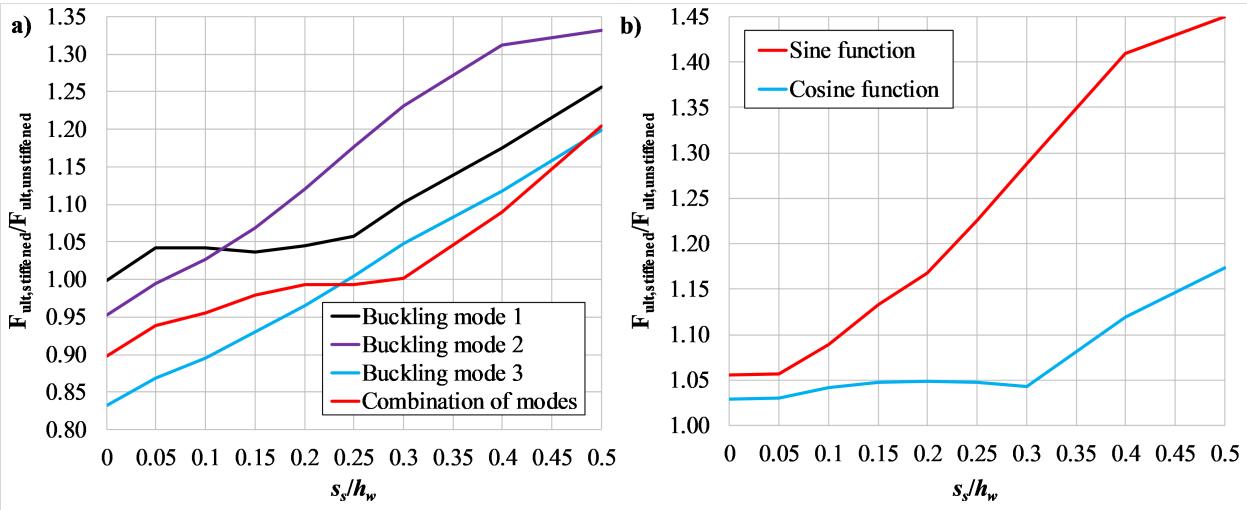

Fig. 20. Comparison of the ultimate strengths between longitudinally stiffened $F_{ult,stiffened}$ and unstiffened $F_{ult,unstiffened}$ girders using as geometrical imperfections: (a) buckling modes; (b) sine and cosine function.

Describing the initial imperfections with sine and cosine function proves the aforementioned conclusions. Again, there is a threshold before which the influence of the longitudinal stiffener has a negligible impact on the ultimate capacity, Fig. 20b. A similar increase in patch load resistance for short patch load lengths was reported by (Loaiza, et al., 2018)

Additionally, the minimum and maximum values for unstiffened and stiffened girders using the experimentally measured imperfections (cf. Fig. 19) are juxtaposed with the buckling-mode based and function-based imperfections. Interestingly, the ultimate load for unstiffened girders considering the experimentally measured imperfections are bounded by ultimate load using the buckling mode-based imperfections (second mode and the combination of modes), Fig. 21a. On the other hand, the ultimate load for stiffened girders considering the experimentally measured imperfections are bounded by ultimate capacity using buckling mode-based and function-based imperfections (third mode and sine function), Fig. 21b. Based on this figure, we can see that the lower band (third buckling mode) is valid for all patch load lengths $s_s/h_w \leq 0.4$ while for $s_s/h_w=0.5$ the lower band is the second buckling mode.

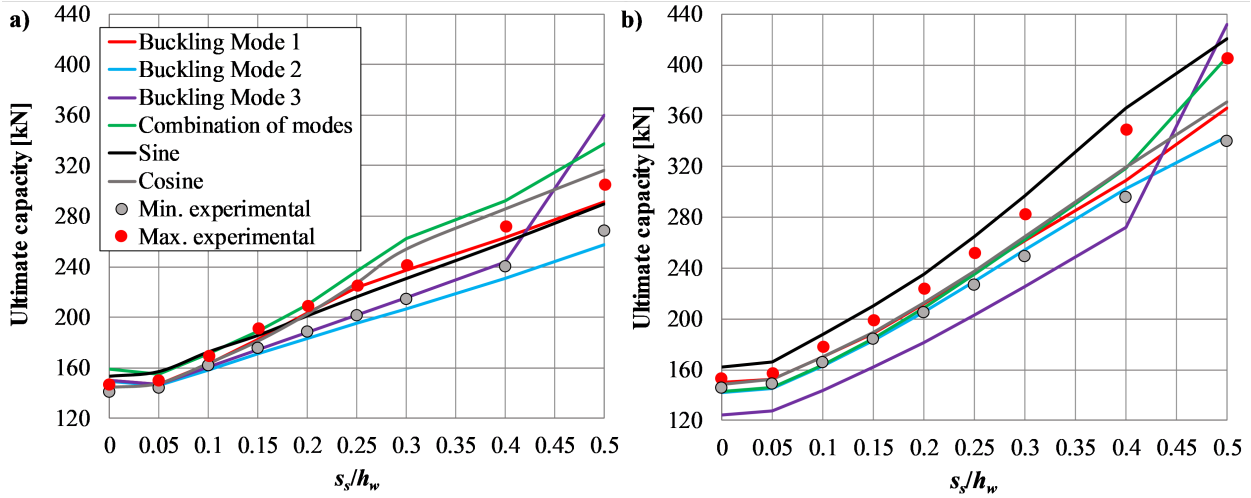

Fig. 21. Ultimate capacity using different initial geometrical imperfections for: (a) unstiffened girders; (b) stiffened girders

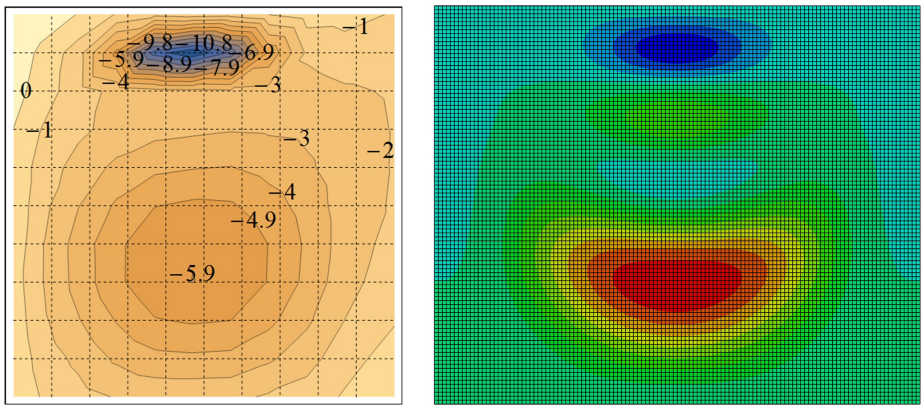

Fig. 22. The deformed shape at collapse from the experiment (left) and the third buckling mode (right) for girder A5 (s_s=100 mm)

The reason that the lowest ultimate capacities for stiffened girders are obtained for the third buckling mode is the fact that this buckling mode corresponds to the deformed shape at collapse load, Fig. 22. As it can be seen, the pronounced deformation is dominant between the longitudinal stiffener and loaded flange and it leads to the lowest ultimate resistance. Using Fig. 13 and isolating only the second and third buckling mode for s_s=200 and 250 mm (s_s/h_w=0.4 and

s_s/h_w=0.5), it can be noticed that for s_s=250 mm the pronounced deformation in the third mode is not anymore between the longitudinal stiffener and loaded flange. In this area, the web panel is practically straight, Fig. 23. Also, we noticed that for this patch load length, the third buckling mode is not symmetric. This change in the initial geometrical imperfection produces much higher ultimate loads and the lowest ultimate strengths are now obtained for the second buckling mode, which has the most unfavorable initial geometrical imperfection for s_s=250 mm. One can argue that these ultimate loads are underestimated and that these initial geometrical imperfections should be scaled differently but our analysis shows that if these imperfections are allowed, they will lead to notably smaller patch load resistances.

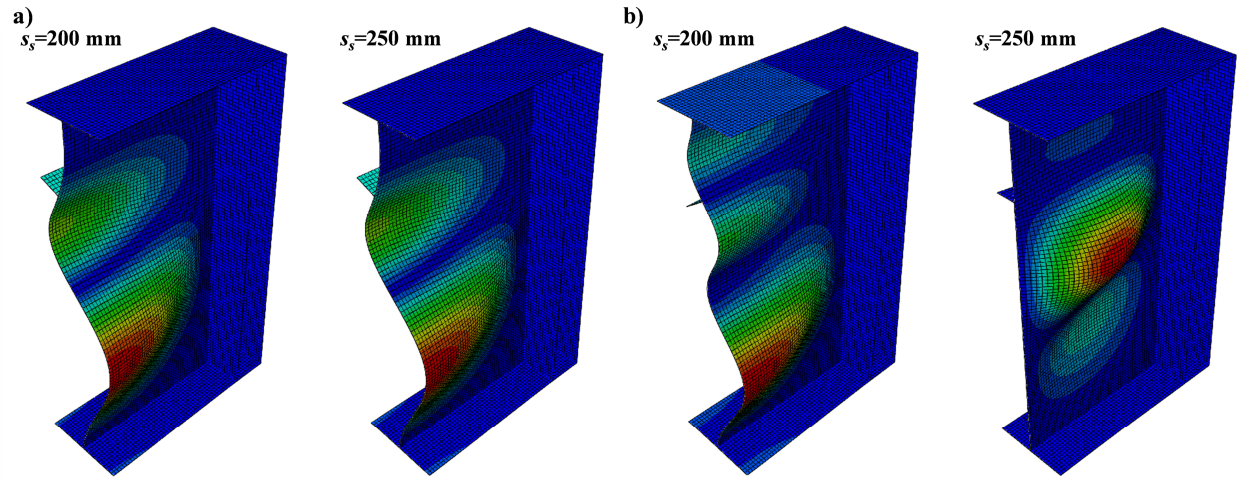

Fig. 23. a) Second buckling mode; b) Third buckling mode

In a nutshell, it may be stated that initial geometrical imperfections can play a decisive role, especially for stiffened girders. Initial geometrical imperfections of stiffened girders that correspond to the deformed shape at collapse (collapse-affine imperfections), especially in the zone where the load is applied, will give the most unfavorable ultimate strengths. *Therefore, it is less important how initial geometrical imperfections are defined (buckling-mode or function-based) but where the deformation is more pronounced*. For this particular case presented in this paper, it turns out that the third buckling mode of stiffened girders corresponds to the deformed shape and the lowest ultimate strengths are obtained.

5. Conclusions

The main finding from this analysis shows that for smaller patch load lengths the longitudinal stiffener has a negligible impact on the ultimate strength. Thus, it can be disregarded from the analysis inasmuch as it increases the patch load resistance of less than 5%. Apparently, this threshold is a function of initial geometrical imperfections and different values are obtained for the experimentally measured imperfections, buckling modes, sine and cosine function based-imperfections. When a specific patch load length (threshold) is reached, an appreciable strengthening effect can be obtained. This can be represented as a magnification factor in which a separation point is the obtained threshold. However, in order to propose an expression for practical use, a further set of studies is required since the present analysis is exclusively based on the same geometrical and material characteristics.

Additionally, it is shown that the initial geometric imperfections can play a decisive role in. According to our parametric study, the lowest ultimate strengths for stiffened girders are obtained using initial geometrical imperfections that correspond to the deformed shape at collapse (collapse-affine imperfections). We have restricted our attention to geometry used in the experiment and for more general conclusions, an additional parametric analysis is highly indispensable. Our future work will consider the effects of girder geometry, material characteristics and aspect ratio of web plate, both experimentally and numerically.

References

Abaqus Simulia. (2016). Dassault Systemes.

EC3 Part 1-5. (2006). Eurocode 3. EN 1993-1-5. Design of steel structures. Part 1-5: Plated structural elements. CEN.

ANSI/AISC. (2016). Specification for Structural Steel Buildings. Chicago, Illinois: American Institute of Steel Construction.

Bergfelt, A. (1979). "Patch loading on a slender web. Influence of horizontal and vertical web stiffeners on the load carrying capacity." Göteborg, Sweden: Department of Structural Engineering, Chalmers University of Technology, Publ. S 79:1.

Bergfelt, A. (1983). "Girder web stiffening for patch loading." Göteborg, Sweden: Department of Structural Engineering, Chalmers University of Technology, Publication S 83:1.

Carretero, A., Lebet, J. (1998). "Introduction des forces concentre´es dans les poutres e´lance´es." *Construction Métallique,*1, 5-18.

Chacon, R., Bock, E., Real, E. (2011). "Longitudinally stiffened hybrid steel plate girders subjected to patch loading." *Journal of Constructional Steel Research,* 67, 1310-1324.

Chacon, R., Bock, M., Mirambell, E., Real, E. (2012a). "Hybrid steel plate girders subjected to patch loading." *Steel Construction,* 5(1), 3-9.

Chacon, R., Mirambell, E., Real, E. (2009). "Influence of designer-assumed initial conditions on the numerical modelling of steel plate girders subjected to patch loading." *Thin-Walled Structures,* 47(4), 391-402.

Chacon, R., Mirambell, E., Real, E. (2010). "Hybrid steel plate girders subjected to patch loading, Part 2: Design proposal." *Journal of Constructional Steel Research,* 66, 709-715.

Chacon, R., Serrat, M., Real, E. (2012b). "The influence of structural imperfections on the resistance of plate girders to patch loading." *Thin-Walled Structures,* 53, 15-25.

Davaine, L. (2005). "Formulation de la résistance au lancement d'une âme métallique de pont raidie longitudinalement." Doctoral thesis. Rennes, France: INSA.

Dogaki, M., Murata, M., Nishijima, Y., Okumura, T., Yonezawa, H. (1991). "Ultimate strength of plate girders with longitudinal stiffener under patch loading." *Technology Reports of Kansai University,* No. 33, 121-132.

Dubas, P., Tschamper, H. (1990). "Stabilité des âmes soumises à une charge concentrée et à une flexion globale." *Construction Métallique,* 2, 25-39.

Galea, Y., Godart, B., Radouant, I., Raoul, J. (1987). "Test of buckling of panels subject to in-plane patch loading." *Proceedings of the ECCS Colloquium on Stability of Plate and Shell Structure,* Ghent University Ghent, 65-71

Graciano, C. (2002). "Patch loading. Resistance of longitudinally stiffened steel girder webs." Doctoral thesis. Luleå, Sweden: Department of Civil and Mining Engineering. Division of Steel Structures. Luleå University of Technology.

Graciano, C., Casanova, E. (2005). "Ultimate strength of longitudinally stiffened I-girder webs subjected to combine patch loading and bending." *Journal of Constructional Steel Research,* 61, 93-111.

Graciano, C., Casanova, E., Martinez, J. (2011). "Imperfection sensitivity of plate girder webs subjected to patch loading." *Journal of Constructional Steel Research,* 67, 1128-1133.

Graciano, C., Edlund, B. (2002). "Nonlinear FE analysis of longitudinally stiffened girder webs under patch loading." *Journal of Constructional Steel Research,* 58, 1231-1245.

Granath, P. (1997). "Behavior of slender plate girders subjected to patch loading." *Journal of Constructional Steel Research,* 42(1), 1-19.

Granath, P., Lagerqvist, O. (1999). "Behavior of girder webs subjected to patch loading." *Journal of Constructional Steel Research,* 50, 49-69.

Janus, K., Karnikova, I., Skaloud, M. (1988). "Experimental investigation into the ultimate load behaviour of longitudinally stiffened steel webs under partial edge loading." *Acta Technica ČSAV*, 2, 158-195.

Kovacevic, S., Markovic, N., Sumarac, D., Salatic, R. (2019). "Influence of patch load length on plate girders. Part II: Numerical research." *Journal of Constructional Steel Research,* revised manuscript submitted.

Kövesdi, B. (2018). "Patch loading resistance of slender plate girders with longitudinal stiffeners." *Journal of Constructional Steel Research,* 140, 237-246.

Kuhlmann, U., Seitz, M. (2004). "Longitudinally stiffened girder webs subjected to patch loading." *Steelbridge 2004*, Millau, France, 1-14.

Lagerqvist, O. (1995). "Patch loading. Resistance of steel girders subjected to concentrated forces." Doctoral thesis. 1994:159D. Luleå, Sweden: Department of Civil and Mining Engineering. Division of Steel Structures. Luleå University of Technology.

Loaiza, N., Graciano, C., Casanova, E. (2018). "Design recommendations for patch loading resistance of longitudinally stiffened I-girders." *Engineering Structures,* 171, 747-758.

Lucic, D. (2003). "Experimental research on I- girders subjected to eccentric patch loading." *Journal of Constructional Steel Research,* 59(9), 1147-1157.

Maiorana, E., Pellegrino, C., Modena, C. (2009). "Imperfections in steel girder webs with and without perforations under patch loading." *Journal of Constructional Steel Research* 65, 1121-1129.

Markovic, N., Hajdin, N. (1992). "A contribution to the analysis of the behaviour of plate girders subjected to patch loading." *Journal of Constructional Steel Research,* 21, 163-173.

Markovic, N., Kovacevic, S. (2019). "Influence of patch load length on plate girders. Part I: Experimental research." *Journal of Constructional Steel Research,* revised manuscript submitted.

Oxfort, J. (1983). "Versuche zum Beul- und Krüppelverhalten von unversteiften Trägerstegblechen unter zentrischen und exzentrischen Einzellasten auf dem Obergurt." *Stahlbau,* 52(10), 309-312.

Rhinoceros 3D. (2018). Robert McNeel & Associates.

Riks, E. (1979). "An incremental approach to the solution of snapping and buckling problems." *International Journal of Solids and Structures,* 15, 529-551.

Roberts, T. (1981a). "Slender plate girders subjected to edge loading." *Proceedings of the Institution of Civil Engineers*, Part 2, pp. 805-819.

Roberts, T. (1981b). Stocky and stiffened plate girders subjected to edge loading. University College Cardiff, Dept. Civil and Struc. Eng., Int. Report.

Roberts, T., Markovic, N. (1983). "Stocky plate girders subjected to edge loading." *Proc. Instn. Civ. Engrs. Technical Note 352. Part 2,* 75, 539-550.

Rockey, K., Bergfelt, A., Larsson, L. (1978). "Behaviour of longitudinally reinforced plate girders when subjected to in plane patch loading." Chalmers University of Technology, Division of Steel and Timber Structures, Publication S78:19, Göteborg.

Salkar, R. (1992). "Strength and behavior of webs, with and without stiffeners under local compressive in-plane and eccentric loads (volumes I and II)." Doctoral thesis. University of Maine, USA.

Salkar, R., Salkar, A., Davids, W. (2015). "Crippling of webs with partial-depth stiffeners under patch loading." *Engineering Journal, AISC,* 52(4), 221-231.

Seitz, M. (2005). "Tragverhalten längsversteifter Blechträger unter quergerichteter Krafteinleitung." Doctoral thesis. Stuttgart: Institut für Konstruktion und Entwurf der Universität Stuttgart.

Shimizu, S., Yoshida, S., Okuhara, H. (1987). "An experimental study on patch-loaded web plates.: *ECCS Coll. on Stability of Plate and Shell Structures,* Ghent University

Walbridge, S., Lebet, J. (2001). "Patch loading tests of bridge girders with longitudinal web stiffeners." *Publication No. 447. Ecole Polytechnique Federale de Lausanne*, Lausanne.